JCTC Journal of Chemical Theory and Computation

Letter

pubs.acs.org/JCTC

Using Force-Matched Potentials To Improve the Accuracy of Density Functional Tight Binding for Reactive Conditions

Nir Goldman,*[,†] Laurence E. Fried,[†] and Lukasz Koziol[†,‡]

[†]Physical and Life Sciences Directorate, Lawrence Livermore National Laboratory, Livermore, California 94550, United States

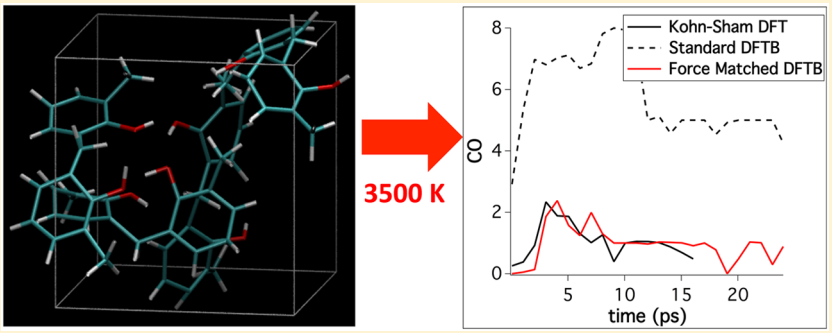

ABSTRACT: We show that force matching can be used to determine accurate empirical repulsive energies for the density functional tight binding method (DFTB) for chemical reactivity in condensed phases. Our approach yields improved results over previous parametrizations for molten liquid carbon and a phenolic polymer under combustion conditions. The method we present here allows for predictions of chemical properties over longer time periods than accessible via Kohn−Sham density functional theory while retaining its accuracy.

Understanding chemical synthesis in the laboratory can require the investigation of a great number of permutations of different starting materials, thermodynamic conditions, and catalysts. The number of possible combinations can frequently be too numerous and costly to address with experimental trial and error alone. Quantum molecular dynamics (MD) simulations hold promise as an independent route to determining the equation of state and chemical reactivity during dynamic processes.[1−4] The density functional tight binding method (DFTB) is a semiempirical quantum simulation approach that yields a high degree of computational efficiency while potentially retaining the accuracy of the computationally intensive Kohn−Sham density functional theory (DFT).[5] DFTB utilizes a minimal local atomic basis set and computes electronic states from a two-center Hamiltonian, which is based on expansion of the Kohn−Sham DFT energy to second order in charge fluctuations. Double counting terms from DFT and ion−ion repulsions are grouped together in a single "repulsive energy" term E_{rep}, which is generally computed through short-range empirical potentials.[6−8] The empirical nature of E_{rep} allows DFTB to be "tuned" to specific physical and/or chemical properties such as isothermal compression curves or small cluster data, frequently computed from DFT as well. These approximations conceivably allow for the study of chemical properties on the nanosecond time scales of experiments at extreme conditions,[9] up to several orders of magnitude longer than what is feasible with standard DFT calculations. However, recent DFTB simulations of phenolic resin pyrolysis have shown that one such parametrization in widespread use (mio-0-1, available for download from http://dftb.org) yields H ion concentrations that are somewhat low and CO production that is significantly too high relative to DFT,[10,11] calling into question the use of these models for simulations under reactive conditions without further verification and/or parameter set development.

One avenue for improving the accuracy of DFTB is through use of the force-matching technique. This approach maximizes the data set that can be obtained from DFT by fitting parameters of a potential function to each individual atomic force in an MD trajectory,[12] yielding a large quantity of data points for determining atomistic models (i.e., $3N$ data points per configuration, where N is the number of atoms in the system). Force matching thus has potential to systematically determine E_{rep} functions that yield highly accurate DFTB predictions of chemical reactivity for a given material or mixture and set of thermodynamic conditions. The method has been used to determine classical force fields for a number of different systems,[13] and has even been applied to a small number of semiempirical approaches other than DFTB.[14,15] However, to date force matching has largely been limited to unreactive systems, and it has not been used explicitly to study more complex reactivity, such as that found in hydrocarbons under reactive conditions.

In this work, we create force-matched DFTB repulsive energy models based on short time scale DFT-MD trajectories. We examine two different systems: liquid metallic carbon at 5000 K and phenolic resin under combustion conditions of

Received: August 3, 2015

DOI: 10.1021/acs.jctc.5b00742
J. Chem. Theory Comput. XXXX, XXX, XXX−XXX

3500 K (Figure 1). All DFT calculations used for these purposes were performed with the VASP code.[16−18] Forces

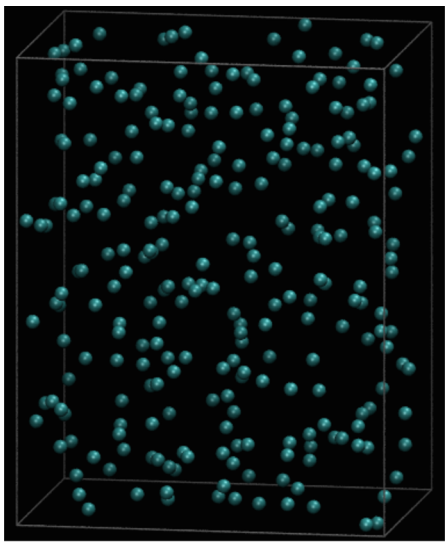

(a) Liquid carbon

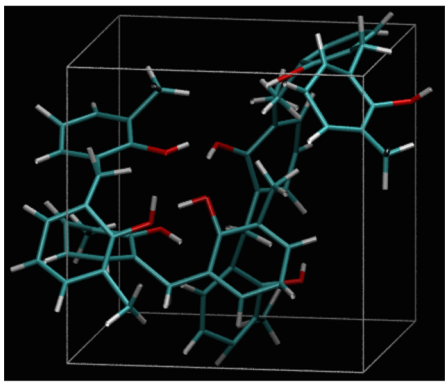

(b) Phenolic resin

Figure 1. MD snapshots of the liquid carbon and phenolic resin simulation cells. Light blue corresponds to carbon, red to oxygen, and white to hydrogen.

from a 5 ps liquid carbon trajectory were used from previous work,[19] which simulated 256 carbon atoms using projector-augmented wave pseudopotentials,[20,21] the Perdew−Burke−Ernzerhof generalized gradient approximation functional (PBE),[22] and a planewave cutoff of 900 eV. Similar to previous studies,[10] phenolic polymer trajectories were computed with the Perdew−Wang functional,[23] ultrasoft pseudopotentials,[24] and a planewave cutoff of 400 eV. This simulation cell contained a total of 132 atoms (four phenolic molecules) with dimensions set to 10.65 × 10.65 × 10.65 Å^3, corresponding to a density of 1.25 g/mL (e.g., a typical room temperature hydrocarbon resin density). One trajectory at 3500 K was run for approximately 15 ps (long enough to determine initial chemical reactivity), though only the first 9 ps were used for our force-matching efforts. A time step of 0.1 fs was required to keep the drift in the conserved quantity in this simulation below 1 kcal/mol/atom. An additional MD trajectory at 3500 K using the highly accurate but more computationally intensive PAW pseudopotentials and the PBE functional yielded virtually identical average system pressures and initial decomposition chemistry. For all systems in this study, cell lattice vectors were large enough to permit Γ-point sampling only of the Brillouin zone.

Each separate force-matching data set was obtained by first taking atomic coordinates and forces from the corresponding DFT trajectory at 100 fs intervals. This amounted to approximately 50 configurations for liquid carbon and 90 for the phenolic polymer. The corresponding DFTB forces from the band structure and electrostatic energies were then computed using the DFTB+ code[25] with the repulsive energies set to zero. The difference from the DFT total atomic forces in each direction were used to determine the force components for the repulsive energy parameters. Previous work has shown that use of self-consistent charge equilibration (SCC)[5] has little effect on the energetics and forces of homoatomic systems such as carbon extreme conditions.[4,7,19] Hence, DFTB forces for liquid carbon were computed using the non-SCC version of the method, only. In contrast, the forces from the phenolic polymer trajectory were computed using SCC convergence to 10^{-6} atomic units (au) due to the fact that in heteroatomic systems the differing electronegativities between atom types require equilibration of the charges.

For our purposes, we represented the repulsive energy by the pairwise ninth-order polynomial,

$$V(r_{ij}) = \begin{cases} \sum_{n=2}^{9} c_n (r_c - r_{ij})^n, & r_{ij} < r_c \\ 0, & \text{otherwise} \end{cases} \quad (1)$$

Here, the c_n correspond to a total of eight linear polynomial coefficients, and r_c ensures that $V(r_{ij})$ and its derivatives smoothly approach zero at a predefined radial cutoff. In this work, each r_c was held fixed at a value that corresponded approximately to the first minimum in the radial distribution function (RDF) for that given atomic pair. The linear dependence of $V(r_{ij})$ on the c_n coefficients allows for use of singular value decomposition (SVD) linear least-squares fitting. Optimum parameter values can then be determined in a single step, thereby removing the need for direct gradient minimization or iterative techniques (e.g., Levenberg−Marquardt) which can become trapped in a local minimum, or computationally intensive global energy minimum searches (e.g., simulated annealing).

It is important to note that a perfectly forced-matched repulsive energy function (i.e., root-mean-square or RMS error of zero) can still result in incorrect values for the system pressure from DFTB. The pressure for a system under periodic boundary conditions can be expressed as follows:[26,27]

$$P = \frac{Nk_bT}{V} + \left\langle \frac{1}{3V} \sum_{i=1}^{N} \mathbf{r}_i \cdot \mathbf{F}_i - \frac{\partial U}{\partial V} \right\rangle \quad (2)$$

Here, N is the number of particles in the system, U is the potential energy, V is the volume, and $\mathbf{r}_i$ and $\mathbf{F}_i$ are the position of and force acting on atom i, respectively. The term $\partial U/\partial V$ is due to the dependence of the potential energy on box size without scaling of atomic coordinates. In the case of a pairwise additive potential energy function, the pressure can be written in terms of pairwise forces as

$$P = \frac{Nk_bT}{V} + \left\langle \frac{1}{3V} \sum_{i=1}^{N-1} \sum_{j=i+1}^{N} \mathbf{r}_{ij} \cdot \mathbf{F}_{ij} \right\rangle \quad (3)$$

DOI: 10.1021/acs.jctc.5b00742
J. Chem. Theory Comput. XXXX, XXX, XXX−XXX

However, for DFTB the atomic forces are not strictly pairwise additive, and the volume dependence of the potential energy cannot be excluded due to the dependence of the charge density on the system volume.

In order to investigate this situation, we have determined two different force-matched potentials for liquid carbon (Table 1):

Table 1. Polynomial Parameters in Atomic Units for the Force-Matched Interaction Potentials for Carbon[a]

parameter	forces only	forces and stress tensor
c_2	-1.1964×10^{-1}	-6.1289×10^{-2}
c_3	5.2690×10^{-1}	3.6179×10^{-1}
c_4	-1.1624	-8.9547×10^{-1}
c_5	1.5168	1.2529
c_6	-1.1914	-1.0333
c_7	5.6259×10^{-1}	5.0859×10^{-1}
c_8	-1.4525×10^{-1}	-1.3662×10^{-1}
c_9	1.5931×10^{-2}	1.5654×10^{-2}

[a]Both models used a radial cutoff of r_c = 3.9684 bohr.

one that is matched only to the interatomic forces (referred to as "forces only") and a second that includes both forces as well as the required diagonal components of the system stress tensor. The linear dependence of the stress tensor from $V(r_{ij})$ on the c_n parameters allows for matching of the stress tensor components to be included in our linear least-squares calculations. For this work, instantaneous stress tensor values were matched in units of GPa, as opposed to au for the forces, which yielded an additional weighting for these data points of 29421 (the approximate conversion factor from au to GPa). Our forces only model yielded an RMS error of 14.98 (kcal/mol)/Å, whereas the potential with stresses yielded an RMS error in the forces of 16.55 (kcal/mol)/Å, and an RMS error in the diagonal stress tensor components of 0.76 GPa.

We have examined our force-matched potentials by conducting *NVT* simulations of liquid carbon at 5000 K with a time step of 0.5 fs for ∼20 ps using Nose−Hoover thermostat chains.[28,29] Analysis of the RDFs shows nearly exact agreement for the first peak from DFT and the forces only model (Figure 2). The model with matched stresses yields a slightly lower first peak, though this difference is relatively small. Both force-matched models yield improvement over our previous carbon E_{rep} parametrization to the diamond cold compression curve,[6] which yields a first peak that is significantly shorter and at too small a distance. The peaks corresponding to the second and third coordination shells from both models in this work agree with those from DFT as well, though their results are slightly more structured, and our previous E_{rep} determination yields slightly better agreement. Predictions for the RDF could be improved through use of a longer cutoff radius which include interactions from these solvation shells. We compute an average system pressure from the forces only model of 8.7 GPa, compared to that of 13.7 GPa from DFT and 12.0 GPa from our model with stresses included. Our approach of including components of the stress tensor in the fitting data set thus strikes a balance between improving the structural properties from an E_{rep} parametrization while including physical properties that would otherwise be neglected.

In order to examine the transferability of the model with stresses included, we have computed the bulk modulus, B_0 (resistance to isotropic compression), for diamond from a Vinet equation of state fitting[30] of the zero temperature

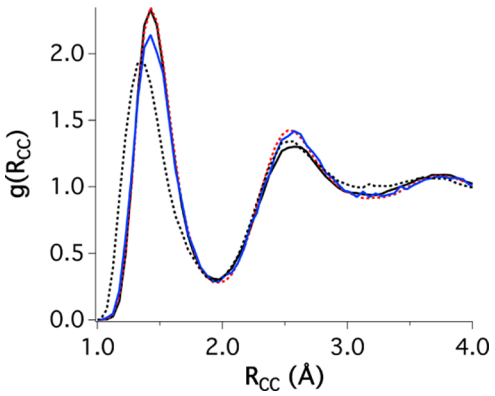

Figure 2. Radial distribution functions for molten carbon at 1500 K and 2.43 g/mL. The solid black line corresponds to results from DFT, the dashed black line to results from a recent DFTB model with dispersion corrections,[19] the red dashed line to our force-matched model using the interatomic forces only, and the solid blue line to our force-matched model using both forces and the diagonal component of the stress tensor. Including the stress tensor components in our data improved the predicted value of the pressure from our simulations while yielding only small differences in the first peak of the RDF.

compression curve up to 140 GPa. Results from this E_{rep} model yield a B_0 value of 480.2 GPa, compared to the experimental result of 446 GPa[31] and that from DFT of 421.0 GPa.[6] Hence, our model with stresses included yields a reasonable degree of transferability to different phases and thermodynamic conditions.

Force-matching results for the phenolic polymer system are shown in Table 2. In this case, our focus was on improving the predictions of decomposition chemistry from DFTB, and we have not included stress tensor matching in these calculations. Previous simulations have shown that no O−O bonds are created at combustion-like temperatures (e.g., 2000−3500 K),[10] in part due to the low concentration of oxygen in this system. Consequently, these interactions were excluded from our force-matching calculations in order to avoid potentially unphysical parametrizations (e.g., E_{rep} with attractive forces), and the O−O repulsive energy from the mio-0-1 parameter set was used instead. All five of the remaining interatomic interactions (C−C, C−O, C−H, O−H, and H−H) were determined simultaneously through our force-matching procedure. The production of small molecules was then monitored during the course of a 20 ps *NVT* simulation at 3500 K with a time step of 0.1 fs (Figure 3), with simulations repeated with mio-0-1 for the sake of consistent simulation parameters. In particular, the excessive CO production from mio-0-1 is rectified in our force-matched model, which replicates the time scale and quantity of CO production from DFT fairly closely. In addition, our force-matched model predicts a more accurate time for the onset of H_2O production, whereas the result from mio-0-1 is somewhat delayed and starts only after 10 ps. However, all three simulations appear to yield similar concentrations over longer time scales. Our model improves somewhat over mio-0-1 for H ion production, which appears to predict a decrease in the overall ion concentration at longer time scales. However, at times less than 10 ps, our force-matched model predicts a slightly lower H ion concentration than DFT.

We have determined a general picture for the ensuing carbon bond chemistry by computing the number of C−C bonds present in each simulation as a function of time. Our results

DOI: 10.1021/acs.jctc.5b00742
J. Chem. Theory Comput. XXXX, XXX, XXX−XXX

Table 2. Polynomial Parameters in Atomic Units for the Phenolic Polymer

parameter	C−C	C−O	C−H	O−H	H−H
r_c	3.9684	3.5905	3.2125	3.4015	2.0787
c_2	-1.0333×10^{-1}	2.2632×10^{-2}	-1.0680×10^{-1}	-5.2828×10^{-3}	-2.5755×10^{-1}
c_3	5.2626×10^{-1}	5.3386×10^{-1}	5.7241×10^{-1}	3.6053×10^{-1}	1.9771
c_4	−1.1504	−2.5634	−1.7066	−1.2259	−8.7740
c_5	1.4196	5.4296	2.9705	2.1765	2.3351×10
c_6	−1.0437	−6.2003	−3.0776	−2.1443	-3.6877×10
c_7	4.6477×10^{-1}	3.9944	1.8936	1.1922	3.4283×10
c_8	-1.146×10^{-1}	−1.3561	-6.3544×10^{-1}	-3.5010×10^{-1}	-1.7319×10
c_9	1.2216×10^{-2}	1.8932×10^{-1}	8.9801×10^{-2}	4.2520×10^{-2}	3.6764

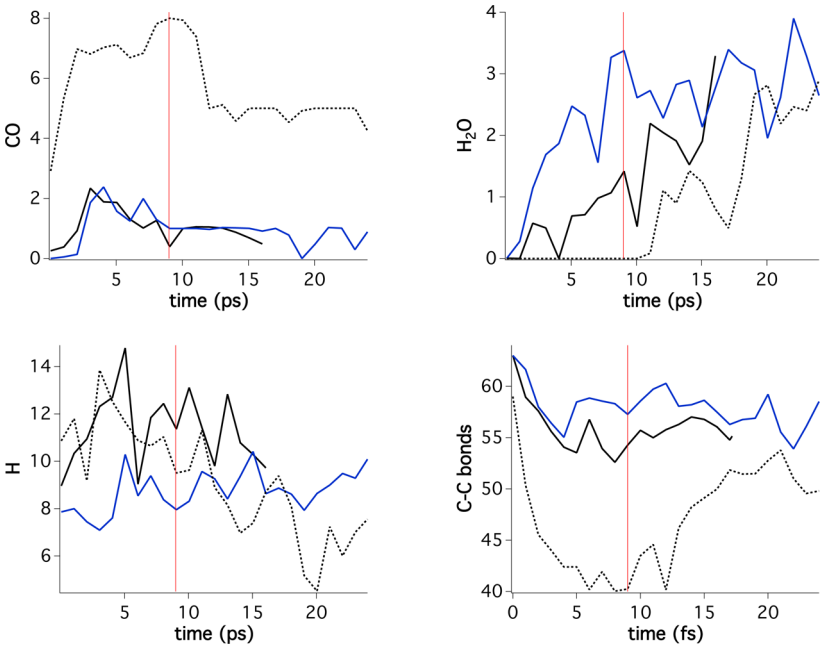

Figure 3. Numbers of specific chemical species from the phenolic polymer at 3500 K, averaged over 1 ps windows. The solid black line corresponds to results from DFT, the dashed line to mio-0-1, and the solid blue line to our interaction potentials from force matching to the first 9 ps of the DFT trajectory (marked by thin red line). Results from our potentials extrapolate to longer time scales.

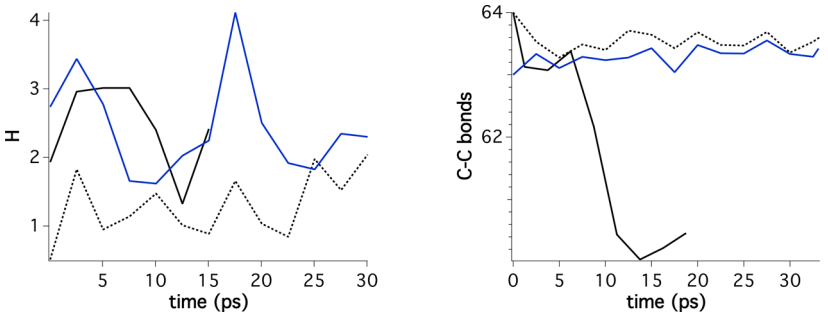

Figure 4. Numbers of hydrogen ions and C−C bonds from the phenolic polymer at 2500 K, averaged over 2.5 ps windows. The solid black line corresponds to results from DFT, the dashed line to mio-0-1, and the solid blue line to our interaction potentials from force-matching fit to a DFT trajectory at 3500 K. Our potential indicates some degree of transferability to different thermodynamic conditions. .

indicate that the mio-0-1 simulation yields too rapid dissociation of C−C bonds, where their total number has decreased by approximately one-third after only 5 ps. In contrast, both DFT and force-matched model yield a much slower decrease in concentration, with only ∼15% of the total number of bonds dissociating over the course of our simulations.

We have examined the transferability of our C−H−O force-matched repulsive energies by simulating the same phenolic polymer system at 2500 K (Figure 4), which was included in the original DFTB study.[10] Simulations with all three methods were run for a minimum of 20 ps using a time step of 0.25 fs. The overall decomposition chemistry is much slower at these conditions, and our DFT simulations yielded the production of single H_2O and CO molecules, which we did not observe from mio-0-1 or our force-matched parameterization on these time scales. Nonetheless, our force-matched model has improved agreement with DFT for H ion production (∼2−3 ions) over

DOI: 10.1021/acs.jctc.5b00742
J. Chem. Theory Comput. XXXX, XXX, XXX−XXX

mio-0-1 at time scales under 20 ps, with both sets of DFTB simulations yielding similar results thereafter. However, both mio-0-1 and our force-matched potentials yield very similar C−C bond chemistry, with dissociation of only a single C−C bond over the course of our simulations, whereas DFT yields dissociation of approximately four C−C bonds after the first 10 ps of simulation. Determination of improved force-matched repulsive energies for reactive chemistry through fitting to larger data sets with more complex representations of E_{rep} is the subject of future work.

Ultimately, our force-matching approach provides a straightforward method for improving the accuracy of DFTB, particularly for chemical reactivity at a given thermodynamic state point, though we do observe some degree of transferability to different conditions. Inclusion of stress tensor matching allows for improved predictions of the system pressure as well without significantly diminishing the accuracy of the interatomic forces. Our methods can be used to extend quantum simulations to closer to equilibrium time scales, where short DFT trajectories can be used to create highly accurate DFTB models that can access 100s of ps or longer. These types of models will have particular use in studies of decomposition of energetic materials[32] or even prebiotic synthesis within astrophysical materials,[33,34] where chemical reactivity can span nanoseconds, and experiments rely on theoretical predictions for possible chemical products.

AUTHOR INFORMATION

Corresponding Author

*E-mail: ngoldman@llnl.gov.

Present Address

‡ExxonMobil Research and Engineering, 1545 Route 22 East, Annandale, NJ 08801, USA.

Funding

This work was performed under the auspices of the U.S. Department of Energy by Lawrence Livermore National Laboratory under Contract DE-AC52-07NA27344.

Notes

The authors declare no competing financial interest.

ACKNOWLEDGMENTS

Computations were performed at Lawrence Livermore National Laboratory using the Aztec and RZMerl massively parallel computers.

REFERENCES

(1) Manaa, M. R.; Reed, E. J.; Fried, L. E.; Goldman, N. Nitrogen-rich heterocycles as reactivity retardants in shocked insensitive explosives. *J. Am. Chem. Soc.* **2009**, *131*, 5483−5487.

(2) Goldman, N.; Reed, E. J.; Fried, L. E. Quantum corrections to shock hugoniot temperatures. *J. Chem. Phys.* **2009**, *131*, 204103.

(3) Goldman, N.; Reed, E. J.; Fried, L. E.; Kuo, I.-F. W.; Maiti, A. Synthesis of glycine-containing complexes in impacts of comets on early Earth. *Nat. Chem.* **2010**, *2*, 949−954.

(4) Goldman, N. Multi-center semi-empirical quantum models for carbon under extreme thermodynamic conditions. *Chem. Phys. Lett.* **2015**, *622*, 128−136.

(5) Elstner, M.; Porezag, D.; Jungnickel, G.; Elsner, J.; Haugk, M.; Frauenheim, T.; Suhai, S.; Seifert, G. Self-consistent-charge density-functional tight-binding method for simulations of complex materials properties. *Phys. Rev. B: Condens. Matter Mater. Phys.* **1998**, *58*, 7260−7268.

(6) Goldman, N.; Fried, L. E. Extending the Density Functional Tight Binding Method to Carbon Under Extreme Conditions. *J. Phys. Chem. C* **2012**, *116*, 2198−2204.

(7) Goldman, N.; Srinivasan, S. G.; Hamel, S.; Fried, L. E.; Gaus, M.; Elstner, M. Determination of a density functional tight binding model with an extended basis set and three-body repulsion for carbon under extreme pressures and temperatures. *J. Phys. Chem. C* **2013**, *117*, 7885−7894.

(8) Srinivasan, S. G.; Goldman, N.; Tamblyn, I.; Hamel, S.; Gaus, M. Determination of a density functional tight binding model with an extended basis set and three-body repulsion for hydrogen under extreme thermodynamic conditions. *J. Phys. Chem. A* **2014**, *118*, 5520−5528.

(9) Martins, Z.; Price, M. C.; Goldman, N.; Sephton, M. A.; Burchell, M. J. Shock synthesis of organics from simple ice mixtures. *Nat. Geosci.* **2013**, *6*, 1045−1049.

(10) Qi, T.; Bauschlicher, C. W.; Lawson, J. W.; Desai, T. G.; Reed, E. J. Comparison of ReaxFF, DFTB, and DFT for phenolic pyrolysis. 1. Molecular dynamics simulations. *J. Phys. Chem. A* **2013**, *117*, 11115−11125.

(11) Bauschlicher, C. W.; Qi, T.; Reed, E. J.; Lenfant, A.; Lawson, J. W.; Desai, T. G. Comparison of ReaxFF, DFTB, and DFT for phenolic pyrolysis. 2. Elementary reaction paths. *J. Phys. Chem. A* **2013**, *117*, 11126−11135.

(12) Ercolessi, F.; Adams, J. B. Interatomic potentials from first-principles calculations: The force-matching method. *Europhys. Lett.* **1994**, *26*, 583−588.

(13) Izvekov, S.; Parrinello, M.; Burnham, C. J.; Voth, G. A. Effective force fields for condensed phase systems from *ab initio* molecular dynamics simulation: A new method for force-matching. *J. Chem. Phys.* **2004**, *120*, 10896−10913.

(14) Lenosky, T. J.; Kress, J. D.; Kwon, I.; Voter, A. F.; Edwards, B.; Richards, D. F.; Yang, S.; Adams, J. B. Highly optimized tight-binding model of silicon. *Phys. Rev. B: Condens. Matter Mater. Phys.* **1997**, *55*, 1528−1544.

(15) Welborn, M.; Chen, J.; Wang, L.-P.; Van Voorhis, T. Why many semiempirical molecular orbital theories fail for liquid water and how to fix them. *J. Comput. Chem.* **2015**, *36*, 934−939.

(16) Kresse, G.; Hafner, J. Ab initio molecular dynamics for liquid metals. *Phys. Rev. B: Condens. Matter Mater. Phys.* **1993**, *47*, 558−561.

(17) Kresse, G.; Hafner, J. *Ab initio* molecular dynamics simulation of the liquid-metal-amorphous-semiconductor transition in germanium. *Phys. Rev. B: Condens. Matter Mater. Phys.* **1994**, *49*, 14251−14271.

(18) Kresse, G.; Furthmüller, J. Efficient iterative schemes for ab initio total-energy calculations using a plane-wave basis set. *Phys. Rev. B: Condens. Matter Mater. Phys.* **1996**, *54*, 11169−11186.

(19) Cannella, C.; Goldman, N. Carbyne fiber synthesis within evaporating metallic liquid carbon. *J. Phys. Chem. C* **2015**, DOI: 10.1021/acs.jpcc.5b03781.

(20) Blöchl, P. E. Projector augmented-wave method. *Phys. Rev. B: Condens. Matter Mater. Phys.* **1994**, *50*, 17953−17979.

(21) Kresse, G.; Joubert, D. From ultrasoft pseudopotentials to the projector augmented-wave method. *Phys. Rev. B: Condens. Matter Mater. Phys.* **1999**, *59*, 1758−1775.

(22) Perdew, J. P.; Burke, K.; Ernzerhof, M. Generalized gradient approximation made simple. *Phys. Rev. Lett.* **1996**, *77*, 3865−3868.

(23) Perdew, J. P.; Chevary, J. A.; Vosko, S. H.; Jackson, K. A.; Pederson, M. R.; Singh, D. J.; Fiolhais, C. Atoms, molecules, solids, and surfaces: Applications of the generalized gradient approximation for exchange and correlation. *Phys. Rev. B: Condens. Matter Mater. Phys.* **1992**, *46*, 6671−6687.

(24) Vanderbilt, D. Soft self-consistent pseudopotentials in a generalized eigenvalue formalism. *Phys. Rev. B: Condens. Matter Mater. Phys.* **1990**, *41*, 7892−7895.

(25) Aradi, B.; Hourahine, B.; Frauenheim, T. DFTB+, a sparse matrix-based implementation of the DFTB method. *J. Phys. Chem. A* **2007**, *111*, 5678−5684 (Note: http://www.dftb-plus.info (accessed Aug. 3, 2015)).

DOI: 10.1021/acs.jctc.5b00742
J. Chem. Theory Comput. XXXX, XXX, XXX−XXX

(26) Louwerse, M. J.; Baerends, E. J. Calculation of pressure in case of periodic boundary conditions. *Chem. Phys. Lett.* **2006**, *421*, 138−141.
(27) Thompson, A. P.; Plimpton, S. J.; Mattson, W. General formulation of pressure and stress tensor for arbitrary many-body interaction potentials under periodic boundary conditions. *J. Chem. Phys.* **2009**, *131*, 154107.
(28) Nosé, S. A unified formulation of the constant temperature molecular dynamics method. *J. Chem. Phys.* **1984**, *81*, 511−519.
(29) Hoover, W. G. Canonical dynamics: Equilibrium phase space distributions. *Phys. Rev. A: At., Mol., Opt. Phys.* **1985**, *31*, 1695−1697.
(30) Vinet, P.; Smith, J. R.; Ferrante, J.; Rose, J. H. Temperature effects on the universal equation of state of solids. *Phys. Rev. B: Condens. Matter Mater. Phys.* **1987**, *35*, 1945−1953.
(31) Occelli, F.; Loubeyre, P.; Letoullec, R. Properties of diamond under hydrostatic pressures up to 140 GPa. *Nat. Mater.* **2003**, *2*, 151−154.
(32) Goldman, N.; Bastea, S. Nitrogen oxides as a chemistry trap in detonating oxygen-rich materials. *J. Phys. Chem. A* **2014**, *118*, 2897−2903.
(33) Goldman, N.; Tamblyn, I. Prebiotic chemistry within a simple impacting icy mixture. *J. Phys. Chem. A* **2013**, *117*, 5124−5131.
(34) Koziol, L.; Goldman, N. Prebiotic hydrocarbon synthesis in impacting reduced astrophysical icy mixtures. *Astrophys. J.* **2015**, *803*, 91−98.

DOI: 10.1021/acs.jctc.5b00742
J. Chem. Theory Comput. XXXX, XXX, XXX−XXX